35th Annual International Conference of the IEEE EMBS
Osaka, Japan, 3 - 7 July, 2013

A Frequency Domain Analysis of Respiratory Variations in the Seismocardiogram Signal

Keya Pandia, Omer T. Inan, Member, IEEE, Gregory T. A. Kovacs, Fellow, IEEE

***Abstract*—The seismocardiogram (SCG) signal traditionally measured using a chest-mounted accelerometer contains low-frequency (0-100 Hz) cardiac vibrations that can be used to derive diagnostically relevant information about cardiovascular and cardiopulmonary health. This work is aimed at investigating the effects of respiration on the frequency domain characteristics of SCG signals measured from 18 healthy subjects. Toward this end, the 0-100 Hz SCG signal bandwidth of interest was sub-divided into 5 Hz and 10 Hz frequency bins to compare the spectral energy in corresponding frequency bins of the SCG signal measured during three key conditions of respiration—inspiration, expiration, and apnea. Statistically significant differences were observed between the power in ensemble averaged inspiratory and expiratory SCG beats and between ensemble averaged inspiratory and apneaic beats across the 18 subjects for multiple frequency bins in the 10-40 Hz frequency range. Accordingly, the spectral analysis methods described in this paper could provide complementary and improved classification of respiratory modulations in the SCG signal over and above time-domain SCG analysis methods.**

Index Terms — seismocardiography, spectral analysis, frequency-domain representation, power spectral density, respiration, apnea, accelerometer.

I. Background and Introduction

The high incidence of cardiovascular disease and its impact on health-care costs in the United States has resulted in a growing need for and interest in affordable home-health monitoring solutions for cardiovascular diagnostics and personalized disease management outside hospital settings [1-3].

Miniature, low-cost MEMS accelerometers have been shown to detect seismocardiogram (SCG) signals that contain features corresponding in timing to cardiac events such as the closing of the mitral and aortic valves [4]. These events, in turn, correspond in timing to the second components of the S1 and S2 primary heart sounds traditionally measured on phonocardiograms. The SCG signals obtained from accelerometers can provide diagnostically relevant information about cardiovascular and respiratory health. In the time-domain, the respiratory modulation of heart sounds results in amplitude and timing changes in the S1 and S2 features of the SCG [5]. The resulting time-domain parameters derived from the SCG have been demonstrated to provide physiologically insightful information about the complex interactions between the cardiovascular and pulmonary systems [5].

This work extends the analysis of the respiratory modulation of the SCG signal by investigating the effect of respiration on the *frequency*-domain representation of the SCG signal. This frequency-domain analysis of the SCG signal provides a complementary approach to the time-domain signal analysis methods for deriving physiologically useful information regarding the complex cardiopulmonary interactions from the SCG signal. Additionally, the use of modern digital signal processing technology to implement these frequency-domain methods could provide improved feature discrimination and classification with simpler circuits.

K. Pandia was supported in part by Texas Instruments, Inc.

K. Pandia and O. T. Inan are with the Department of Electrical Engineering, Stanford University, Stanford, CA, 94305 USA (e-mails: keya.pandia@stanfordalumni.org, oeinan@gmail.com).

G. T. A. Kovacs is with the Department of Electrical Engineering and (by courtesy) the School of Medicine, Stanford University, Stanford, CA 94305 USA (e-mail: kovacs@cis.stanford.edu).

II. Method

A. System Design

The dorso-ventral SCG signal was obtained from human subject volunteers using a miniature MEMS accelerometer (LIS3L02AL, STMicroelectronics, Geneva, Switzerland). The SCG signal was preconditioned using a custom analog front end [5]. A lead-II electrocardiogram (ECG) and a respiration effort belt signal were also acquired concurrently using custom analog electronics and data acquisition system described in [5]. The SCG, ECG, and respiration signals thus acquired were recorded and stored for further processing using custom software (Matlab®, Version 2007b, The Mathworks, Natick, MA).

B. Human Subject Protocol

Twenty healthy human subjects (twelve male, eight female) were recruited for this study under the protocol 6503 approved by the Stanford Institutional Review Board. Data from two subjects (one male, one female) were not considered for this analysis due to poor reference respiration signals in both cases. The subject demographics (mean, standard deviation) were: age (28.9, 5.9 years), height (1.71, 0.11 m), and weight (65.9, 12.8 kg). The accelerometer was taped on the subjects' chests on the left mid-sternal area

along the mid-clavicular line; ECG electrodes were affixed to the subjects' torso to capture a lead-II electrocardiogram signal and a respiration belt was attached to their upper torso to acquire a reference respiration signal. The subjects were asked to sit comfortably in a chair and to breathe normally for 60 seconds followed by a 15 second period of breath hold (apnea).

C. Signal Processing and Signal Analysis

The dorso-ventral SCG signal obtained from the chest-mounted accelerometer was digitally low pass filtered at 100 Hz to limit sensor noise above the frequency range of interest. The SCG signal was then digitally high pass filtered at 0.5 Hz to attenuate the low frequency baseline variation caused by respiratory chest wall movement. Finally, a 60 Hz notch filter was used to eliminate line interference in the SCG signal. The respiration belt signal was low pass filtered at 0.5 Hz; the ECG signal at 50 Hz.

During the first 60 seconds of normal breathing, the respiration signal was used to obtain a mean respiration rate and respiration interval for each subject. The SCG signal was sub-divided into consecutive frames—each frame spanning the duration of the mean respiration interval for the corresponding subject and normalized in amplitude with respect to the maximum amplitude of the signal in the frame. For a given respiration cycle, the S1 heart sound is at its highest amplitude during the expiratory phase and at its lowest amplitude during the inspiratory phase [5-6]. These findings were congruent with time stamps for the start of inspiration and expiration phases annotated by subjects during the course of the measurement. Consequently, for each frame, the SCG beat corresponding to the highest S1 amplitude was used as the expiratory beat for that frame and the beat corresponding to the lowest S1 amplitude was considered the inspiratory beat. For each subject, an ensemble average of expiratory beats was computed by averaging all of the expiratory beats for that subject during the 60 seconds of normal breathing. An ensemble average of inspiratory beats was similarly computed for each subject. The S1 peaks for each frame were detected using an S1 peak detection algorithm described in [7]. Similarly, during the 15 second interval of breath hold (or apnea), for each subject, an ensemble average was computed for all SCG beats during the interval of breath hold.

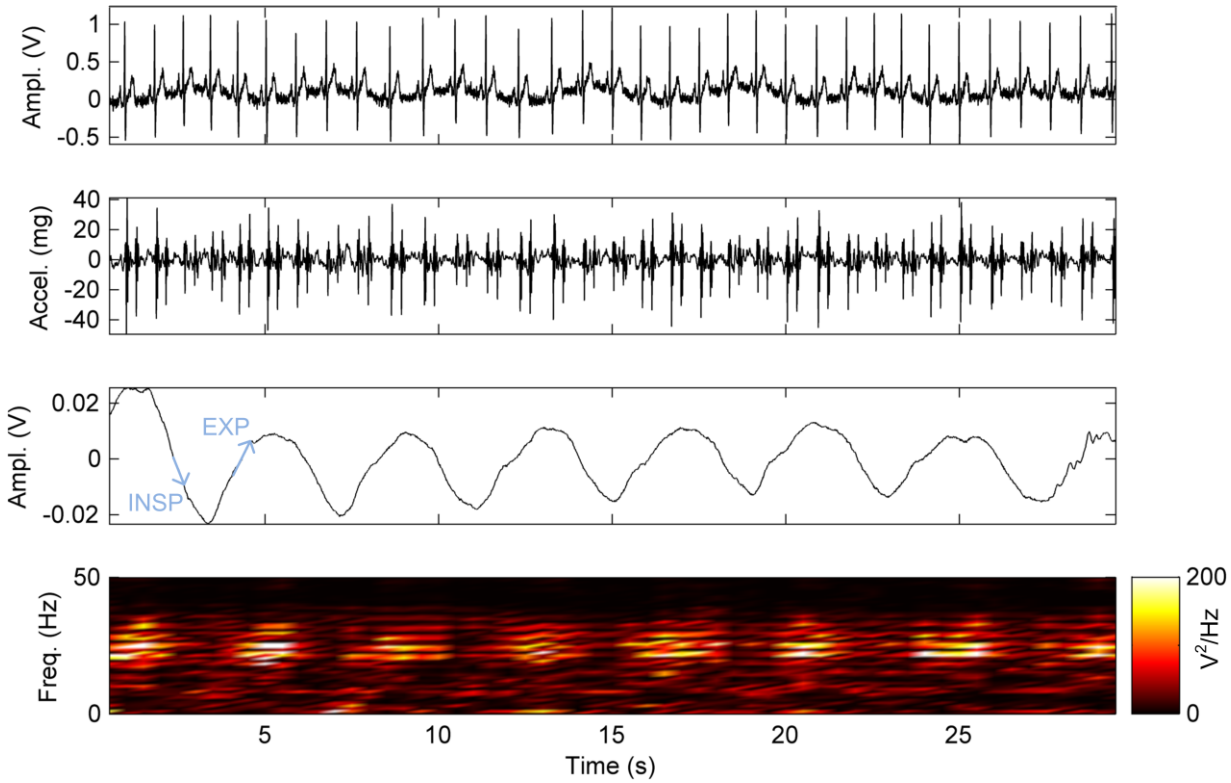

Figure 1: Figure showing 30 seconds of concurrently recorded time traces of an ECG, SCG, and reference respiration belt signal (INSP and EXP represent the start of the inspiratory and expiratory phases as annotated by a subject participating in the study); and a spectrogram (time-frequency representation) of the 30 second recording of the SCG.

A spectrogram plot was constructed for visual analysis of the time-frequency characteristics of the SCG signal during the first 30 seconds of regular breathing. A one second

window with a 0.5 second overlap between windows was used to compute the spectrogram.

Furthermore, a power spectrum of each of the inspiratory, expiratory and apneaic ensemble averaged beats was constructed for every subject. The aggregate power spanning 0-100 Hz was computed with frequency bins spaced 10 Hz apart; similarly, the aggregate power in 5 Hz frequency bins spanning 0-50 Hz was computed for each subject. Finally, a composite measure of power across all 18 subjects was computed by averaging the power in each of the abovementioned corresponding frequency bins for the 18 subjects. The composite power in each of the frequency bins corresponding to the inspiratory phase was then compared to the composite power in the corresponding bins in the expiratory phase and the apneaic phase. The statistical significance of the differences was computed using Student's t-test (threshold of $p < 0.05$, corrected for multiple comparisons using the Holm–Bonferroni method [8]).

III. Results and Discussion

A. Visual Inspection of the Time-Frequency Characteristics of the SCG Signal

The concurrently recorded time traces of the ECG, SCG, and respiration effort belt signals for a single subject during 30 seconds of regular breathing are shown in Figure 1. As shown alongside the time traces, the spectrogram plot of the SCG signal shows modulations in the frequency content of the SCG signal that correlate in periodicity with the respiration belt signal. As evident from Figure 1, the periodic maxima in spectral power coincide in timing with the expiratory phases of the respiration cycles. This finding is congruent with previous results demonstrating maximal S1 amplitude during expiration and minimal S1 amplitude during inspiration [5-6].

B. Visual Inspection of the Signal Ensemble Averages and Power Spectral Densities

As shown in Figure 2, the expiratory ensemble average for a single subject as well as the corresponding power spectral density show greater amplitude and power in the expiratory beat compared to the inspiratory beat. Furthermore, the energy in the apneaic ensemble average is greater than the energy in the inspiratory ensemble average; but is closer to the energy in the expiratory beat ensemble average.

C. Statistical Analysis of the Signal Power Distributions

As shown in Figure 3, the signal ensemble average power for each of the respiratory phases—inspiration, expiration and apnea—is concentrated in the sub-50 Hz frequency range. Accordingly, the signal power in the frequency span from 0-50 Hz was further investigated with a finer (5 Hz) frequency resolution (*see,* Figure 4).

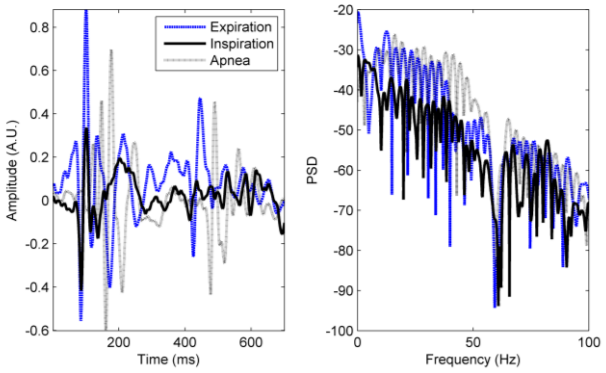

Figure 2: Figure showing ensemble averages and corresponding power spectra obtained for a single subject during inspiration, expiration, and apnea. (The power spectral density is shown in normalized arbitrary units.)

As shown in Figures 3-4, the composite power distribution of the SCG signal across the 18 subjects during the inspiratory phase when compared to each of the expiratory and apneic phases showed statistically significant differences in multiple frequency bins (primarily between 10-40 Hz) spanning the 0-100 Hz frequency range (significant differences relative to the inspiratory beat power for the respective frequency bin are shown with an asterisk in Figure 3). Similarly, significant differences were also observed for multiple frequency bins in the 0-50 Hz frequency range (significant differences relative to the inspiratory beat power for the respective frequency bin are

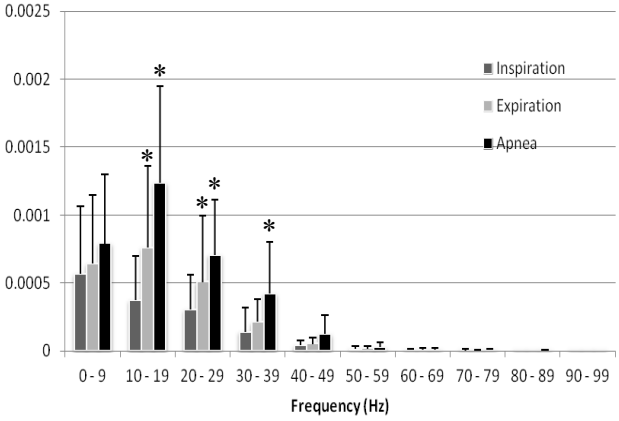

Figure 3: Statistical analysis of spectral energy between 0-100 Hz with 10 Hz frequency spacing measured across the 18 subjects during inspiration, expiration, and apnea. (The Y-axis represents power spectral density in normalized, arbitrary units.)

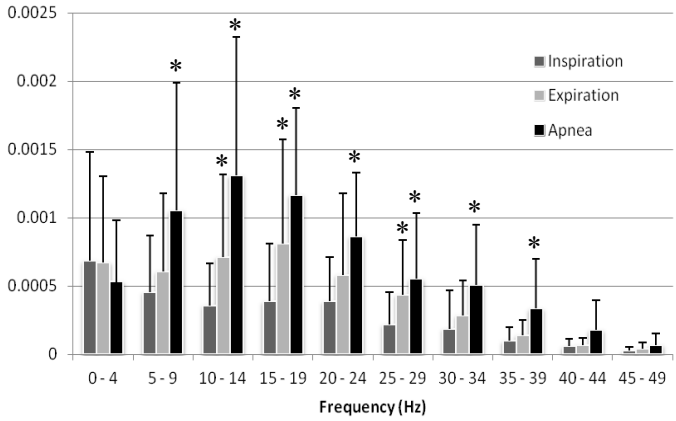

Figure 4: Statistical analysis of spectral energy between 0-50 Hz with 5 Hz frequency spacing measured across the 18 subjects during inspiration, expiration, and apnea. (The Y-axis represents power spectral density in normalized, arbitrary units.)

shown with an asterisk in Figure 4). These findings are in agreement with the power concentration in the periodic expiratory phases as shown in the spectrogram in Figure 1.

Additionally, as illustrated in Figures 3-4, the power spectral density of the inspiratory ensemble average showed a peak in the 0-9 Hz range and the inspiratory beat power was observed to have a decreasing trend with increasing frequency toward 100 Hz. On the other hand, for the expiratory and apneic beats, the power spectral density peaks in the 10-19 Hz range and decreases in the frequency range below 10 Hz and above 20 Hz. Furthermore, the power in the apneaic beats was found to be higher than the corresponding power in the inspiratory or expiratory beats for a majority (9 out of 10 in each case) of the frequency bins considered in the 0-100 Hz frequency range as well as in the 0-50 Hz frequency range.

IV. CONCLUSION AND FUTURE WORK

With an aim to understand the spectral variations in the SCG signal as a function of respiration, this work investigates the spectral power in ensemble averaged SCG beats measured during three key conditions of respiration—inspiration, expiration, and apnea. The ensemble averaged SCG beats measured during each of these three phases across 18 healthy subjects were compared visually in the time-domain and statistically in the frequency-domain to investigate variations in the spectral characteristics of the SCG signal due to respiration.

Statistically significant differences were observed between various frequency components (spectral bins) computed for the inspiratory ensemble average when compared to the corresponding frequency components measured during expiration and during apnea. The power in the ensemble averaged expiratory beat was found to be greater than the power in the ensemble averaged inspiratory beat across the 18 subjects, with the difference being statistically significant for several frequency bins. Furthermore, the spectral energy for the ensemble averaged apneaic beat was significantly greater than the corresponding power in the inspiratory SCG beat for multiple frequency bins in the frequency ranges considered. These results indicate that in addition to the time-domain methods for analyzing and classifying respiratory variations in the SCG signal, the frequency-domain methods described above could provide complementary information regarding the respiratory modulation of the SCG caused by physiologically complex cardio-pulmonary interactions.

Future work will focus on expanding these methods to investigate differences in the respiratory frequency characteristics of the SCG in disease populations (e.g., in patients in cardiovascular, pulmonary, or cardiopulmonary disease) when compared to healthy populations. Furthermore, the effects of inter-subject bias (e.g., due to varying respiration rates across subjects) and sampling bias (e.g., due to the non-uniformity in cardiac timings relative to the respiration waveform) on the computed frequency responses will be investigated.

V. ACKNOWLEDGMENT

The authors are thankful for the financial support provided, in part, through Texas Instruments and the Center for Integrated Systems (CIS).

VI. REFERENCES

[1] C. J. L. Murray, T. Vos, R. Lozano, *et al.*, "Disability-adjusted life years (DALYs) for 291 diseases and injuries in 21 regions, 1990-2010: a systematic analysis for the Global Burden of Disease Study 2010," *The Lancet*, v. 380, pp. 2197-223, 2013.

[2] P. A. Heidenreich, J. G. Trogdon, O. A. Khavjou, *et al.*, "Forecasting the future of cardiovascular disease in the United States: A Policy Statement from the American Heart Association," *Circulation*, v. 123, pp. 933-44, 2011.

[3] A. L. Bui and G. C. Fonarow, "Home monitoring for heart failure management," J Am Coll Cardiol, v. 59, pp. 97-104, 2012.

[4] D. M. Salerno, J. Zanetti, "Seismocardiography for monitoring changes in left ventricular function during ischemia," *Chest*, vol. 100, pp. 991-993, October 1991.

[5] K. Pandia, O. T. Inan, G. T. A. Kovacs, and L. Giovangrandi, "Extracting respiratory information from seismocardiogram signals acquired using a chest-worn accelerometer," *Phys Meas*, v. 33, pp. 1643-60, 2012.

[6] G. Amit, K. Shukha, N. Gavriely, and N. Intrator, "Respiratory modulation of heart sound morphology," *Am J Physiol Heart Circ Physiol*, v. 296, pp. H796-805, 2009.

[7] K. Pandia, S. Ravindran, R. Cole, G. T. A. Kovacs, and L. Giovangrandi, "Motion artifact cancellation to obtain heart sounds from a single chest-worn accelerometer," *ICASSP: IEEE Int. Conf. on Acoustics Speech and Signal Processing Dallas, TX*, pp 590–3, 2010.

[8] S. Holm, "A simple sequentially rejective multiple test procedure," *Scand. J. Stat.,* v. 6 pp. 65–70, 1979.